HW2: Report of Results

Elias Firisa

April 8, 2025

Problem 1a: Determination of I_c for 25 Hz Spiking in the Hodgkin–Huxley Model

In this problem, we implement a Hodgkin–Huxley (HH) model neuron using the parameters provided in the lecture notes (with time in ms, voltage in mV, and current in mA). The model is governed by the equation

$$C\frac{dV}{dt} = I_{\text{ext}} - \Big[I_{\text{Na}} + I_{\text{K}} + I_{\text{L}}\Big],$$

with the ionic currents defined as

$$I_{\text{Na}} = g_{\text{Na}}\, m^3 h\,(V - E_{\text{Na}}), \quad I_{\text{K}} = g_{\text{K}}\, n^4\,(V - E_{\text{K}}), \quad I_{\text{L}} = g_{\text{L}}\,(V - E_{\text{L}}).$$

The gating variables n, m, and h obey first-order differential equations with voltage-dependent rate functions $\alpha_x(V)$ and $\beta_x(V)$.

A constant current I_c is applied starting at $t = 100$ ms (with $I_{\text{ext}} = 0$ for $t < 100$ ms). For a stimulus window from 100 to 500 ms (i.e. 400 ms), a firing rate of 25 Hz corresponds to 10 spikes.

Efficient Determination of I_c

To efficiently determine the value of I_c that yields 25 Hz spiking, we employed a bisection search algorithm. The steps are as follows:

1. **Initial Bracketing:** We set initial bounds $I_{c,\text{low}} = 2\,\mu\text{A/cm}^2$ (which produced 0 spikes) and $I_{c,\text{high}} = 18\,\mu\text{A/cm}^2$ (which produced a high spiking rate).

2. **Target Spikes:** For a 400 ms stimulus, 25 Hz corresponds to 10 spikes.

3. **Bisection:** At each iteration, we compute $I_{c,\text{mid}} = (I_{c,\text{low}} + I_{c,\text{high}})/2$, run the simulation over the interval $[0, 500]$ ms, and count the spikes during the stimulus period (100–500 ms). Depending on whether the spike count is below or above 10, we update the lower or upper bound. This iterative halving of the search interval quickly converges on the optimal I_c.

After 11 iterations, the search converged to an optimal injected current of

$$I_c \approx 6.2148\,\mu\text{A/cm}^2.$$

A final simulation using this current produced exactly 10 spikes in the stimulus window, corresponding to a 25 Hz firing rate.

Figure and Results

Figure 1 shows the membrane potential $V(t)$ as a function of time for $t \in [0, 500]$ ms. The plot demonstrates that the neuron remains at rest before $t = 100$ ms and then fires regularly once the current is applied, yielding 10 spikes in the 400 ms window.

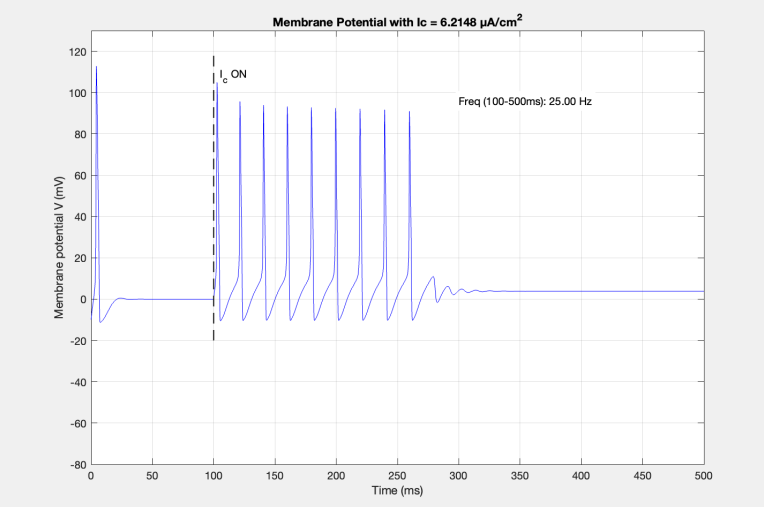

Figure 1: Membrane potential $V(t)$ for $t \in [0, 500]$ ms with a constant injected current $I_c \approx 6.2148\,\mu\text{A/cm}^2$ applied at $t = 100$ ms. The trace shows that the neuron produces 10 spikes during the stimulus window, corresponding to a firing rate of 25 Hz.

The use of a bisection search allowed us to efficiently determine the optimal I_c that induces 25 Hz spiking. This method reduces the number of simulations needed by halving the search interval at each iteration. Our final simulation confirmed that an injected current of approximately 6.2148 μA/cm^2 produces the desired spiking behavior.

Problem 1b: Spike Timing Detection

In this section, we present two methods to detect the spike timing τ of each action potential from the voltage trace obtained in Problem 1(a).

Method 1: Peak Detection This method identifies the spike time as the moment when the membrane potential reaches its maximum during the upstroke of the action potential. Our algorithm operates by first detecting an upward crossing of a predefined threshold (here, $V_{\text{th}} = 0$ mV) and then tracking the voltage until it begins to decrease. The time corresponding to the highest voltage is recorded as the spike time. This approach has the advantage of reflecting a physiologically meaningful event (the spike peak) and is relatively robust to minor fluctuations in the chosen threshold.

Method 2: Simple Threshold Crossing Alternatively, spike timing can be determined by simply detecting the time when the voltage first crosses the threshold $V_{\text{th}} = 0$ mV in the upward direction. This method is computationally very efficient and easy to implement, but it may not accurately reflect the peak of the spike and is more sensitive to the exact threshold value, especially in the presence of noise.

Results and Comparison Using both methods on the voltage trace from Problem 1(a), we obtained identical spike counts (10 spikes in the stimulus period), confirming that both methods capture the same underlying spiking events. However, the measured spike times differ by a few milliseconds: the threshold crossing method typically detects the spike onset earlier (e.g., 112.66, 130.96, 150.08 ms, etc.), whereas the peak detection method identifies the spike peak later (e.g., 121.46, 140.64, 160.10 ms, etc.). This delay is consistent with the physiological delay between the onset of depolarization and the peak of the action potential.

Figure Figure 2 shows the HH model membrane potential $V(t)$ over the interval $[0, 500]$ ms, with red markers indicating the spike times determined by the peak detection method. The overlay confirms that the detected spike peaks align with the maximum depolarization in each spike.

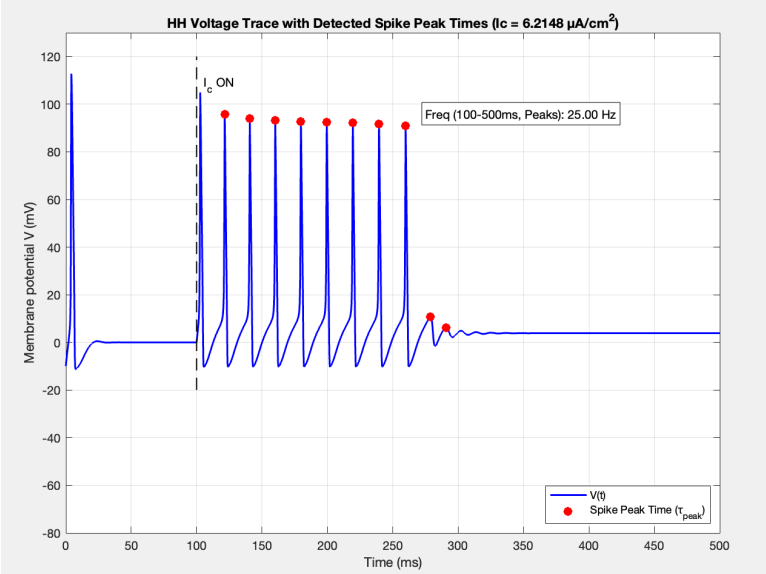

Figure 2: HH model membrane potential $V(t)$ from 0 to 500 ms with detected spike times (red circles) using the peak detection method. Both methods yield 10 spikes; however, the peak detection method records the time of maximal depolarization, which occurs slightly after the initial threshold crossing.

Both spike detection methods successfully extract the spike timings from the HH voltage trace. The peak detection method is preferred for precise determination of the spike peak time, whereas the simple threshold crossing method is computationally simpler. The differences in the detected spike times (approximately 5–10 ms) highlight the sensitivity of the detection method to the definition of "spike time."

Problem 1c: Neuron Response Function and High-Current Behavior

To investigate the neuron's response function, we varied the injected current I_c from 0 to 120 μA/cm^2 and computed the spike count (using our simple threshold-crossing method) during the stimulus period (100–500 ms). Figure 3 shows the resulting f–I curve, where the x-axis represents the injected current and the y-axis indicates the number of spikes within the stimulus window.

The response function exhibits a characteristic "inverted-U" shape. For low currents ($I_c < 5\,\mu$A/cm^2), the neuron remains silent. Once the current exceeds the threshold (approximately 5–6 μA/cm^2), the neuron begins to fire, and the spike count increases steeply, reaching a maximum at moderate currents (e.g., around 75 μA/cm^2). However, as I_c is further increased towards 120 μA/cm^2, the spike count declines back to zero. This drop is due to *depolarization block*, a state where the neuron remains so strongly depolarized that it fails to repolarize adequately, thereby preventing the generation of distinct action potentials.

In addition, at very high currents the shape of the action potentials becomes altered; the peaks are reduced and the waveform can become broadened or flattened. This change in spike morphology can challenge our spike-counting algorithm, which relies on detecting an upward crossing of a fixed threshold (0 mV in our case). Although our simple threshold-crossing method works well for moderate currents where the spikes are clearly defined, it fails in the depolarization block regime because the membrane potential no longer crosses the threshold reliably.

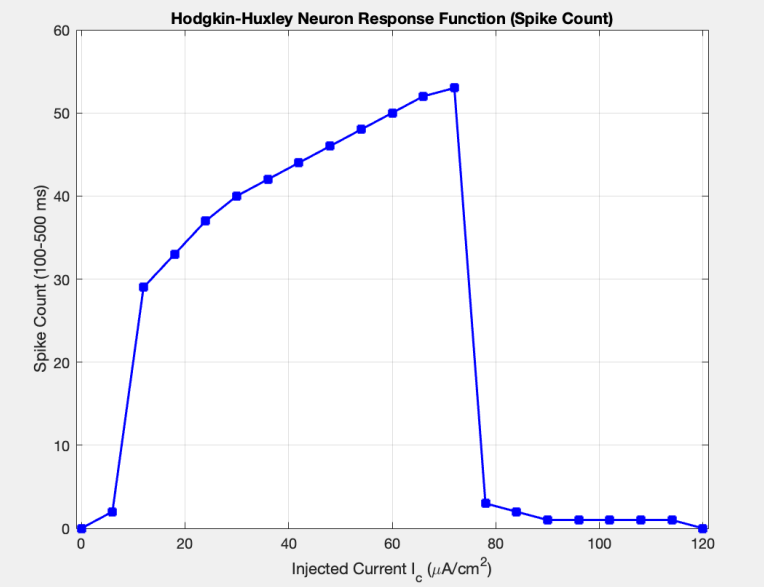

Figure 3: Response function of the HH neuron: Spike count (in the 100–500 ms window) versus injected current I_c (in $\mu\text{A/cm}^2$). The curve shows that the neuron remains silent for low currents, fires robustly at intermediate currents, and then ceases to spike (depolarization block) at very high currents.

Problem 1d: Response Function of LIF Neuron

To compare with the Hodgkin–Huxley model, we implemented a Leaky Integrate-and-Fire (LIF) neuron governed by

$$C_m \frac{dV}{dt} = -g_L(V - V_{\text{rest}}) + I_{\text{ext}},$$

with the following parameters:

[noitemsep]$C_m = 1.0\,\mu\text{F/cm}^2$ $g_L = 0.3\,\text{mS/cm}^2$ $V_{\text{rest}} = -65\,\text{mV}$ $V_{\text{th}} = -55\,\text{mV}$ $V_{\text{reset}} = -70\,\text{mV}$ Absolute refractory period $t_{\text{ref}} = 1\,\text{ms}$

We simulated the neuron from $t = 0$ to $t = 500$ ms, with the stimulus (constant current I_c) starting at $t = 100$ ms. For each value of I_c (ranging from 0 to 70 $\mu\text{A/cm}^2$), we counted the number of spikes during the stimulus period (100–500 ms) using a simple threshold-crossing method. The resulting f–I curve, shown in Figure 4, plots the spike count versus I_c.

Observations: The LIF model produces a smooth, monotonically increasing response function. As I_c increases, the spike count rises continuously until it saturates due to the 1 ms refractory period. In contrast, the Hodgkin–Huxley model (as seen in Problem 1(c)) exhibits a more abrupt transition (type II excitability) and can even enter depolarization block at high currents, leading to a non-monotonic f–I profile.

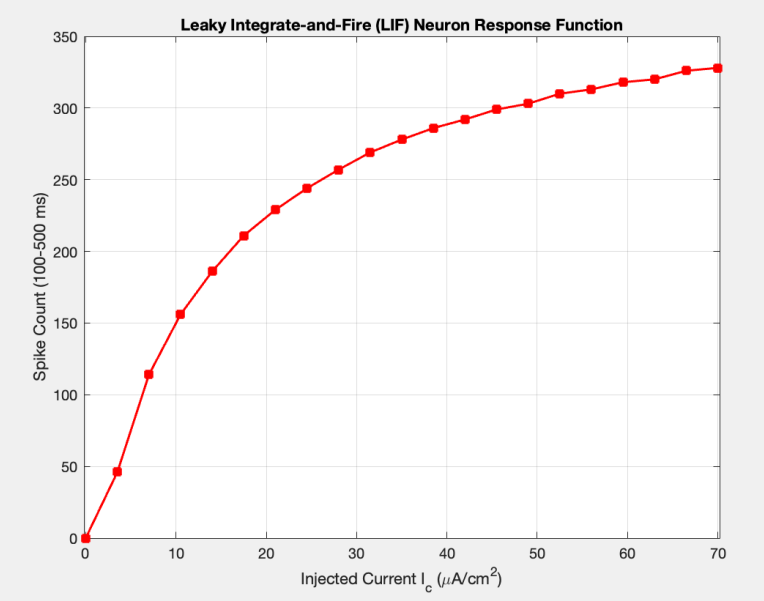

Figure 4: Response function of the LIF neuron: Spike count (in the 100–500 ms window) versus injected current I_c (in $\mu\text{A/cm}^2$). The smooth, monotonic increase in spike count saturates at high currents due to the 1 ms refractory period.

Comparison: The LIF model's response function is notably different from that of the HH model. While the LIF neuron exhibits a continuous increase in firing rate with increasing I_c (limited only by the refractory period), the HH neuron shows a more complex behavior, including a sharp threshold and potential depolarization block at high currents. This comparison highlights how the simplicity of the LIF model results in a smoother f–I curve, whereas the biophysical details in the HH model lead to richer dynamics.

Problem 2a: Plot of spike trains for Ie that produces 25Hz

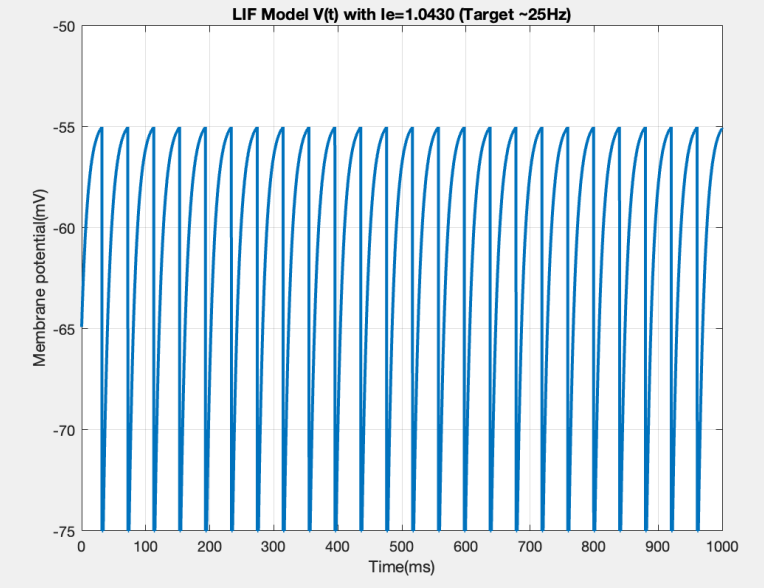

Figure 5: Raster plot illustrating the synchronous firing patterns of two identical LIF neurons. Model parameters were: $C_m = 1.0\,\mu\text{F/cm}^2$, $g_L = 0.1\,\text{mS/cm}^2$, $V_{\text{rest}} = -65\,\text{mV}$, $V_{\text{thresh}} = -55\,\text{mV}$, $V_{\text{reset}} = -75\,\text{mV}$, and $t_{\text{ref}} = 2\,\text{ms}$. Both neurons were driven by a constant current $I_e = 1.0195\,\mu\text{A/cm}^2$, sufficient to elicit a firing rate of approximately 25 Hz over the 1-second simulation.

Problem 2b: Neuron Interactions

To investigate the dynamics of coupled neurons (Problem 2b), the Leaky Integrate-and-Fire (LIF) model developed previously was extended to include synaptic interactions between the two neurons. A conductance-based synapse model was implemented, where a spike in the presynaptic neuron triggers an instantaneous increase (g_{peak}) in the postsynaptic neuron's synaptic conductance (g_{syn}), which then decays exponentially with a time constant (τ_{syn}). This synaptic conductance generates a current

$$I_{\text{syn}} = g_{\text{syn}}\,(V - E_{\text{syn}}),$$

influencing the postsynaptic neuron's membrane potential dynamics.

Two main scenarios were simulated: (i) mutual excitation ($E_{\text{syn}} = 0\,\text{mV}$) and (ii) mutual inhibition ($E_{\text{syn}} = -80\,\text{mV}$). For each scenario, the goal was to achieve specific firing patterns — simultaneous firing (Condition B) and alternating firing (Condition A) — by iteratively adjusting key parameters: the constant input current (I_e), the synaptic strength (g_{peak}), and the synaptic decay time constant (τ_{syn}). The resulting spike trains were visualized using raster plots to evaluate the network behavior. The parameter tuning focused on achieving the most readily expected patterns: synchrony with excitation and alternation with inhibition. The difficulty in stably achieving alternation with excitation or synchrony with inhibition using this simple model was noted.

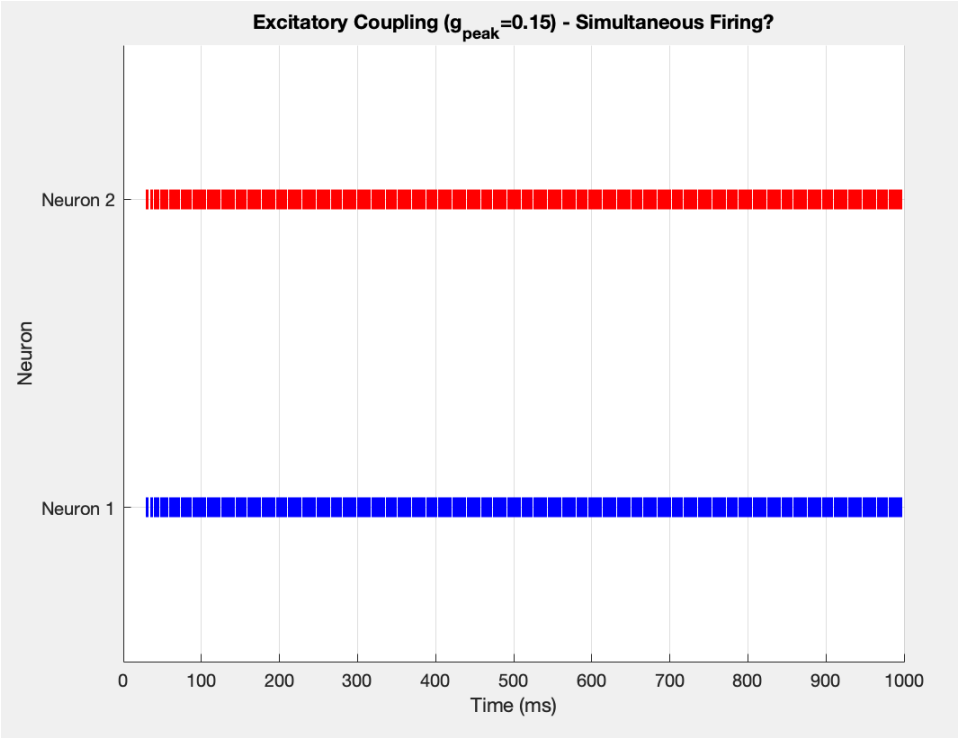

Figure 6: Raster plot showing synchronous firing achieved in a network of two mutually coupled excitatory LIF neurons. The strong positive feedback via excitatory synapses ($E_{\text{syn}} = 0\,\text{mV}$) pulls the neurons into lock-step firing. Parameters used: $I_e = 1.05\,\mu\text{A/cm}^2$, $g_{\text{peak}} = 0.15\,\text{mS/cm}^2$, and $\tau_{\text{syn}} = 5.0\,\text{ms}$. Core LIF parameters are as described in the text (Part 2a). The simulation duration is 1000 ms.

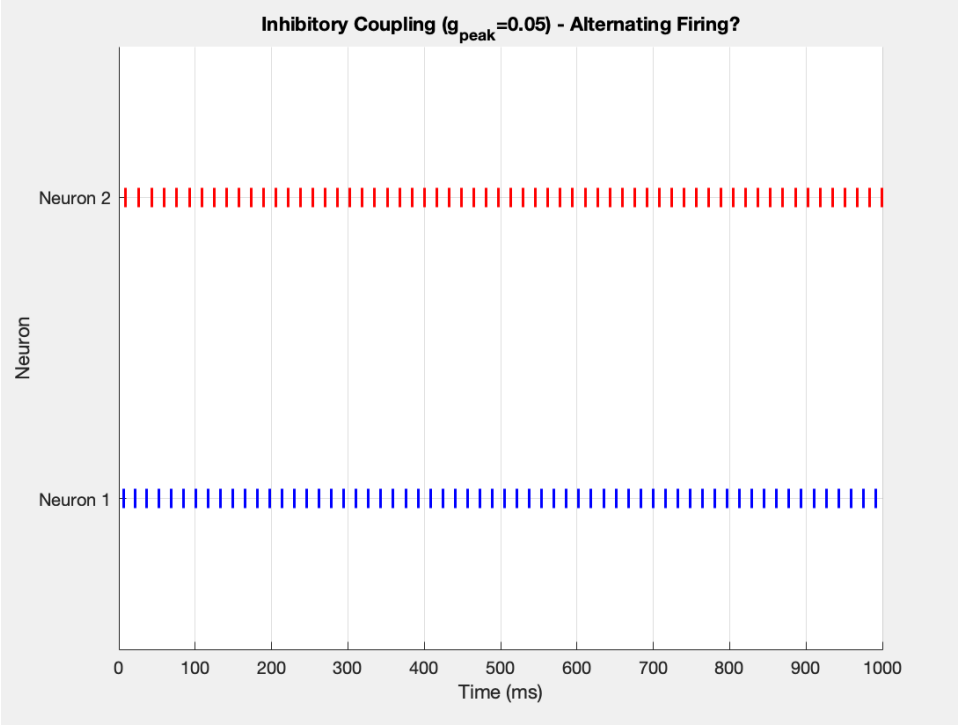

Figure 7: Raster plot showing an alternating (anti-phase) firing pattern achieved in a network of two mutually coupled inhibitory LIF neurons. Mutual inhibition ($E_{\text{syn}} = -80\,\text{mV}$) together with sufficient external drive ($I_e = 2.0\,\mu\text{A/cm}^2$) causes the neurons to transiently suppress each other after firing, resulting in an interleaved spike train. Synaptic parameters used were: $g_{\text{peak}} = 0.05\,\text{mS/cm}^2$ and $\tau_{\text{syn}} = 5.0\,\text{ms}$. Core LIF parameters are as described in the text (Part 2a). The simulation duration is 1000 ms.

Problem 2c: Introducing Gaussian Noise

To model stochastic neuronal firing (Problem 2c), independent Gaussian white noise with zero mean and standard deviation σ was added to the constant baseline input current ($I_e \approx 1.04\,\mu\text{A/cm}^2$, determined in 2a) for each of the two LIF neurons at every time step. Synaptic coupling was disabled ($g_{\text{peak}} = 0$). The standard deviation of the instantaneous firing rate, calculated from the inter-spike intervals (ISIs) over longer simulations (5 s), was used as a measure of firing variability. A numerical search (iterative refinement/bisection) was performed to find the value of σ that resulted in

this standard deviation being approximately equal to the target of 5 Hz. A final 1-s simulation was run using the determined σ value to generate the spike trains.

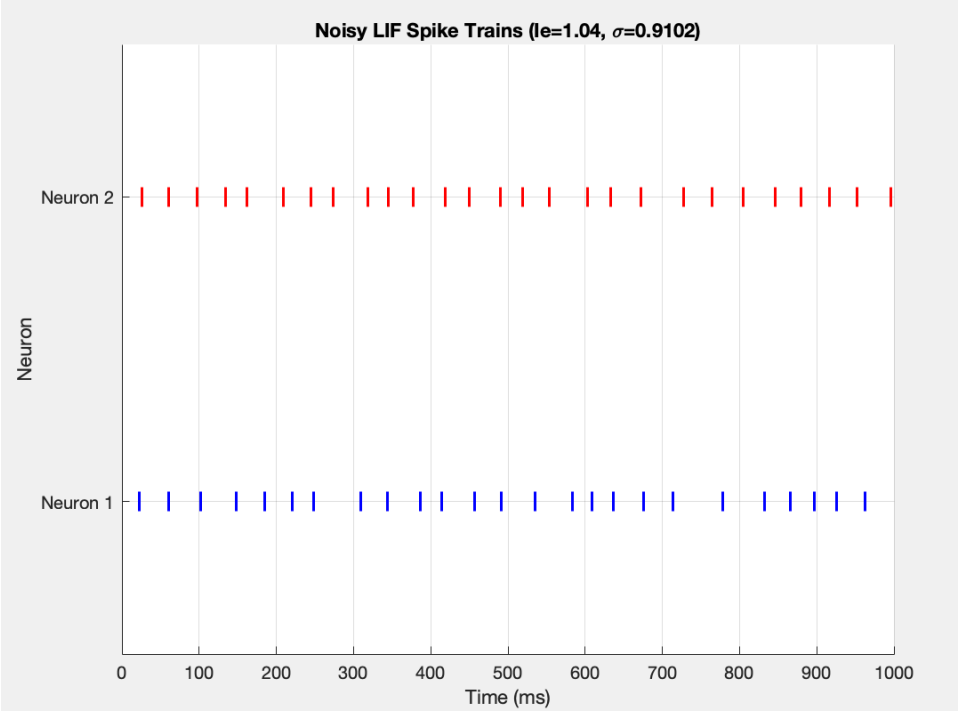

Figure 8: Irregular, independent spike trains from two LIF neurons driven by constant input ($I_e \approx 1.04\,\mu\text{A/cm}^2$) plus independent Gaussian noise ($\sigma \approx 0.9102\,\mu\text{A/cm}^2$). The noise level was selected to produce an approximately 5 Hz standard deviation in the instantaneous firing rate. Note the variability in inter-spike intervals compared to noise-free firing. Simulation duration is 1000 ms.

Problem 2d: Problem 'b' with the Noise

To investigate the effect of noise on coupled neuron dynamics, the simulations from Problem 2b were repeated with the addition of independent Gaussian white noise to each neuron. For these simulations, the LIF neurons received independent noise with zero mean and standard deviation $\sigma \approx 0.91\,\mu\text{A/cm}^2$ (as determined in Problem 2c). This noise current was

added at each time step ($dt = 0.1\,\text{ms}$) to the constant baseline input current I_e. Importantly, the synaptic parameters and the baseline input(Problem 2b) were maintained. The final 1-second simulation was then run with these settings, and the resulting spike trains were visualized using raster plots to assess the effects of the noise on the coupled dynamics.

The addition of independent noise produced distinct effects in the two coupling scenarios:

Excitatory Coupling: Under mutual excitatory coupling (with $E_{\text{syn}} = 0\,\text{mV}$), the strong synchronizing effect inherent in the positive feedback maintained largely synchronous firing, even in the presence of noise. Although the precise timing of the synchronous events became more irregular—resulting in increased variability in inter-spike intervals—the overall pattern remained synchronized (see Figure 9).

Inhibitory Coupling: For mutually inhibitory neurons (with $E_{\text{syn}} = -80\,\text{mV}$), the regular alternating (anti-phase) pattern observed in the noise-free case was significantly disrupted by the noise. The strict anti-phase firing, characterized by a clear interleaving of spikes, was lost as both neurons began to fire irregularly. This indicates that the alternating state, which relies on precise timing of inhibitory feedback, is more sensitive to stochastic fluctuations than the synchronizing effect seen under excitatory interactions (see Figure 10).

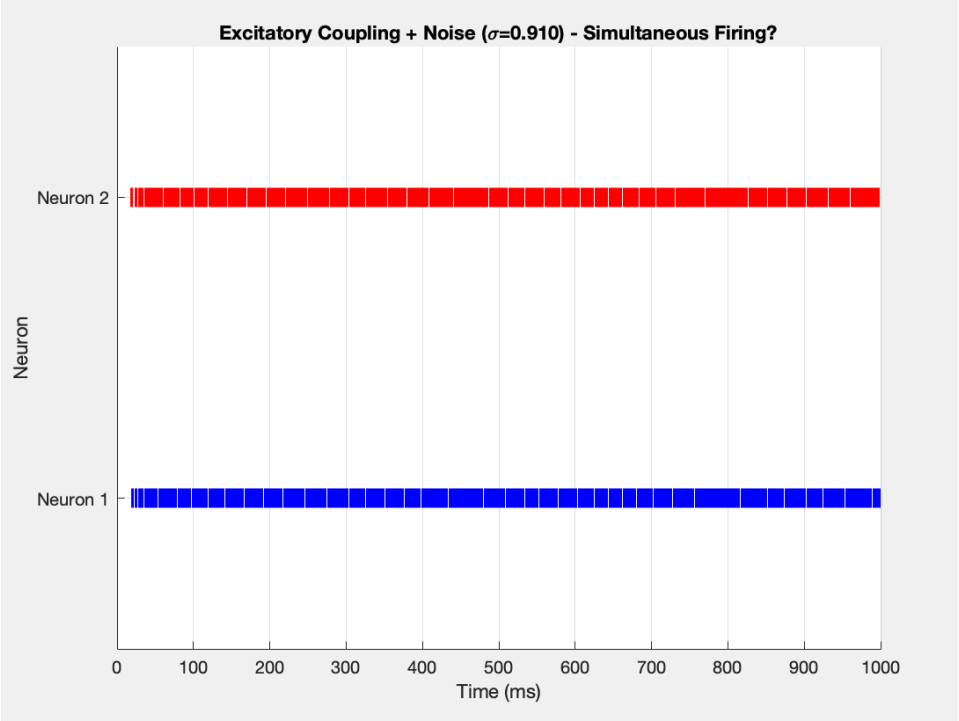

Figure 9: Spike trains of two mutually excitatory LIF neurons with independent noise ($\sigma \approx 0.91\,\mu\text{A/cm}^2$). Synchronous firing is largely maintained compared to the noise-free case, although the timing of synchronous events exhibits increased irregularity. Synaptic and drive parameters are identical to the noise-free synchronous case ($I_e = 1.05\,\mu\text{A/cm}^2$, $g_{\text{peak}} = 0.15\,\text{mS/cm}^2$). The simulation duration is 1000 ms.

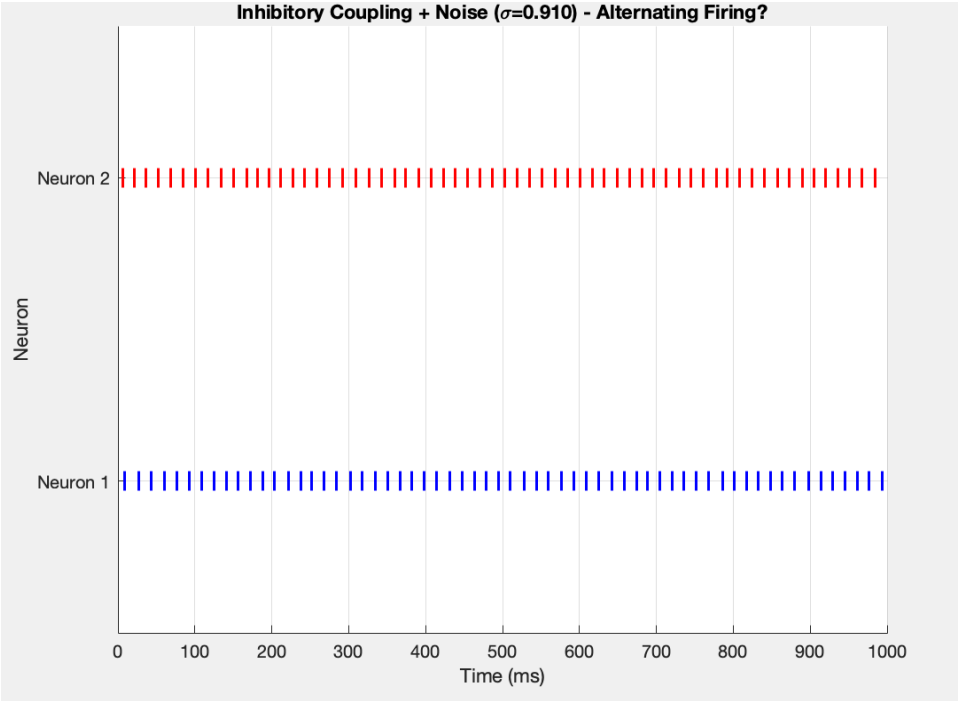

Figure 10: Spike trains of two mutually inhibitory LIF neurons with independent noise ($\sigma \approx 0.91\,\mu\mathrm{A/cm^2}$). The regular alternating firing pattern observed in the noise-free scenario is disrupted, with both neurons firing irregularly and the strict anti-phase relationship lost. Synaptic and drive parameters are identical to the noise-free alternating scenario ($I_e = 2.0\,\mu\mathrm{A/cm^2}$, $g_{\mathrm{peak}} = 0.05\,\mathrm{mS/cm^2}$). The simulation duration is 1000 ms.